Progress In Electromagnetics Research, Vol. 168, 31–38, 2020

A Novel Millimeter-Wave Backward to Forward Scanning Periodic Leaky-Wave Antenna Based on Two Different Radiator Types

Yiming Zhang[1], Hui Liu[1, 2, *], Chenyang Meng[1], Yuxin Lin[1], Yuan Zhang[1], Erik Forsberg[2], and Sailing He[1, 2, 3, *]

Abstract—A periodic millimeter wave leaky-wave antenna (LWA), which has two different types of radiator elements that enable backward to forward radiation, is proposed. The unit-cell of the LWA consists of two quarter-wavelength microstrip lines and two corrugated substrate integrated waveguide (CSIW) cells with S-shaped quarter-wavelength open-circuit stubs. In addition to two parallel edge radiators, a single etched transverse slot with a tilt angle acts as an ancillary radiator, which ensures impedance matching in a large frequency range and achieves the backward to forward scanning. We analyze the proposed design through simulations, characterize a fabricated prototype, and find it to have good radiation properties including broad impedance bandwidth. The measurement results show a high peak gain from 11 to 15.8 dBi with a large scanning angle range from -34° to $+22^\circ$ in the K-band operating frequency range.

1. INTRODUCTION

Radar and satellite systems operating in the K-band are widely used in communication services, and depending on the application, specific antenna design is required. For long distance communication and accurate speed detection, a high gain and narrow beam width antenna is preferred [1, 2]. For these reasons, leaky-wave antennas have attracted much attention due to their high gain, simple feeding structure, unique frequency beam scanning capability, and wide operational bandwidth [3, 4]. A transverse slotted rectangular waveguide, as a simple structure of leaky-wave antenna, was reported by Hyneman in 1959 [5]. Dispersion relations and modes for a dielectric-filled rectangular waveguide with transverse slots were investigated by Liu et al. [6], and their analyses indicate that such a waveguide supports a leaky waveguide mode, a surface-wave mode, and a proper waveguide mode. However, the rectangular waveguide is costly, heavy, and bulky, and the corresponding design for antenna applications in the millimeter-wave (mmW) band is challenging. For this reason, recent focus has been on using a substrate integrated waveguide (SIW) as a dielectric-filled waveguide structure, since this structure has several attractive features such as low cost, low loss, and being easy to integrate with planar circuits [5]. Several types of SIW leaky-wave antennas with transverse slots have been reported [7–9]. Furthermore, the electric fields of microstrip line are evaluated by McMillan et al. [10], and their analyses illustrate that the microstrip transmission line also allows a leaky mode. Lee et al. proposed a method of using a microstrip line to replace the SIW unit-cell delay section, which significantly reduced the length of the periodic and the circularly polarized (CP) periodic LWAs, as well as improved both broadside radiation matching and CP purity [11].

Received 22 July 2020, Accepted 17 September 2020, Scheduled 2 October 2020

* Corresponding author: Sailing He (sailing@kth.se), Hui Liu (liuhuizju@zju.edu.cn).

[1] RF Circuits & Microwave Device Lab, Centre for Optical and Electromagnetic Research, South China Academy of Advanced Optoelectronics, South China Normal University, Guangzhou 510006, China. [2] RF Circuits & Microwave Device Lab, Center for Optical and Electromagnetic Research, National Engineering Research Center for Optical Instruments, Zhejiang University, Hangzhou 310058, China. [3] Ningbo Research Institute, Zhejiang University, Ningbo 315100, China.

Corrugated SIWs (CSIW) utilize a quarter-wavelength open-circuit stub in lieu of the metallic vias used in SIW structures, while retaining equivalent characteristics. In comparison with an SIW structure, the CSIW maintains DC isolation between the top and bottom conductors by use of the open-circuit quarter wavelength stubs, which significantly simplifies the fabrication process [12]. The use of open-circuit quarter wavelength stubs also enables design of tunable LWAs. CSIWs thus have great potential for advanced LWA design, exemplified by e.g., a CP LWA based on a CSIW, with etched slot pair elements on the CSIW top surface, which achieved beam scanning and good axial ratio (AR) in the main beam direction [13]. A high gain millimeter-wave LWA based on a bent corrugated SIW with a large beam angle scanning range from -69° to -10° in the frequency range from 22 to 29.2 GHz [14] and an electronically controlled LWA, which realized beam scanning at a fixed frequency by loading varactor diodes on the CSIW structure [15] were recently reported.

In this paper, we propose a novel periodic slotted leaky-wave antenna for the K-band based on an S-shaped folded CSIW in which wave leakage is achieved using two separate radiating elements, a transverse slot as well as parallel edges cut at the opposite corners of each CSIW cell. In comparison to our previously reported antenna design [14], utilizing the S-shaped folded CSIW and replacing the CSIW delay sections with microstrip lines enables a more compact structure and much larger bandwidth. In addition, the introduction of a tilted transverse slot improves the antenna impedance. This novel design uniquely enables the possibility for backward to forward frequency beam scanning.

2. ANTENNA DESIGN AND ANALYSIS

A top view on the proposed LWA and a detailed view of the unit-cell are depicted in Fig. 1. The structure is based on a Taconic TLY-5-0100 substrate with dielectric constant $\varepsilon_r = 2.2$, loss tangent $\tan\sigma = 0.0009$ and a height h of 0.254 mm. The LWA unit-cell is composed of two microstrip lines of quarter-wavelength length (denoted cell 1 & cell 4 in Fig. 1(b)) and two CISW cells with S-shaped open-circuit stubs (cell 2 & cell 3), in the center of which one transverse slot is etched. The total length of the unit-cell is determined as the corresponding wavelength of the antenna center frequency (f_0). Two diagonal parallel radiation edges connect the microstrip lines and CISW cells (as indicated in Fig. 1(b)). Detailed dimensions of the proposed unit-cell and LWA are summarized in Table 1.

Table 1. Geometry parameters for the proposed LWA.

Symbol	Value	Symbol	Value	Symbol	Value
L_c	2.36 mm	L_f	9.1 mm	L_{f0}	4.6 mm
L_m	2.1 mm	L_s	2.21 mm	L_{st0}	0.47 mm
L_{st1}	0.63 mm	L_{st2}	0.99 mm	L_{cut}	3.65 mm
L_{sub}	160.8 mm	W_c	7.02 mm	W_f	0.88 mm
W_{f0}	0.55 mm	W_m	1.46 mm	W_s	0.59 mm
W_{st}	0.25 mm	W_{sub}	32.0 mm	R_t	0.72 mm
D_{st}	0.84 mm	θ_c	124°	θ_s	118°
p	$(L_m + L_c) \times 2$				

To analyze the performance of the unit-cell, we use dispersion and Bloch impedance diagrams, which can be obtained for the periodic LWA from the S-parameters of the unit-cell:

$$\beta p = \cos^{-1}\left(\frac{1 - S_{11}S_{22} + S_{12}S_{21}}{2S_{21}}\right) \tag{1}$$

$$Z_B = \frac{2jZ_0S_{21}\sin(\beta p)}{(1 - S_{11})(1 - S_{22}) - S_{21}S_{12}} \tag{2}$$

where β is the phase constant, and p is the length of the unit-cell [16–20]. All S-parameters of the unit-cell were extracted using fast driven-mode simulation in Ansys HFSS [19]. The reference impedance

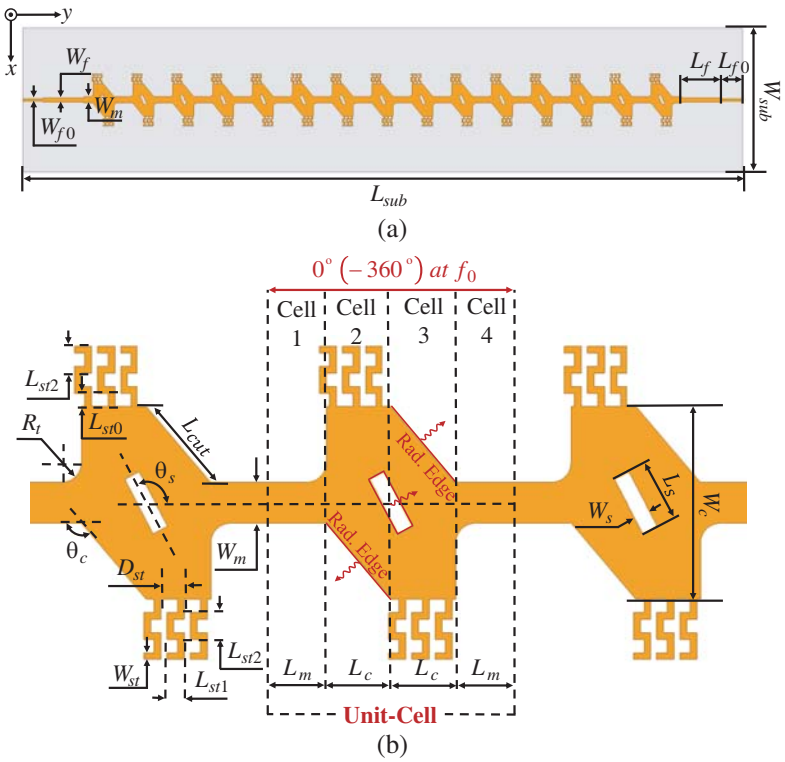

Figure 1. Geometry of the proposed LWA. (a) Top view of the full LWA with 15 unit-cells; (b) 3 unit-cells of the proposed LWA.

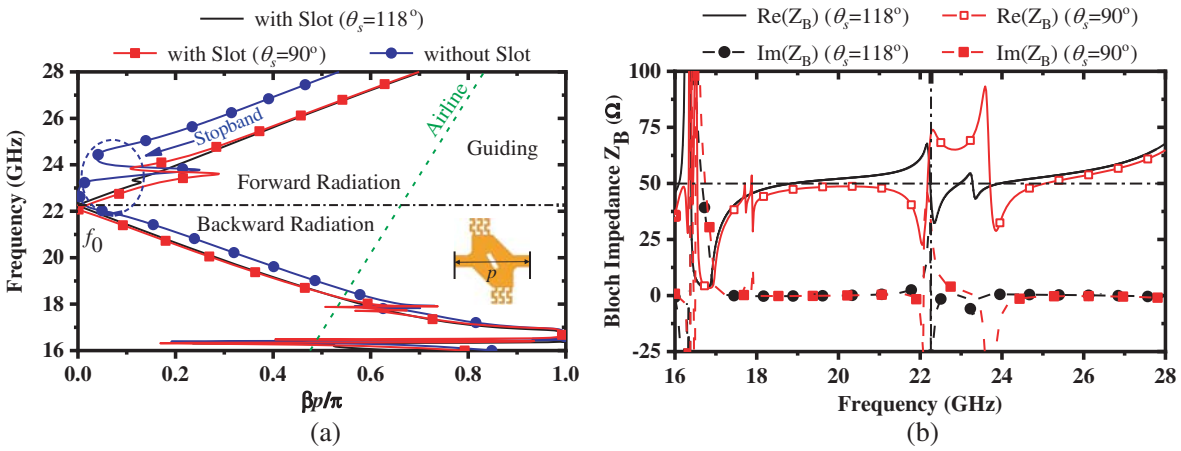

Figure 2. Characteristics of the LWA unit-cell. (a) Dispersion diagram; (b) Bloch impedance.

of the S-matrix, Z_0, is defined as 50 Ω in our design. The calculated dispersion diagram is plotted in Fig. 2(a), where the frequency range is separated into a guiding range and a radiating range as indicated by the plotted airline, the slope of which is $2p \times \text{freq}/c_0$ [18]. The radiating regions are located in the area enclosed by the dispersion curves and the airline. The backward radiation and forward radiation regions are separated by the center frequency f_0, and the broadside radiation is acquired at center frequency f_0. We note that, when the proposed LWA only has edge radiators, a stopband between 22 to 25 GHz can be observed in the region where β is close to zero.

In order to eliminate the stopband to realize continuous backward to forward radiation, a single transverse slot is etched at the center of the unit-cell to act as an additional radiator. The required slot

length can be estimated to be [14, 21]:

$$l = \frac{\lambda_0}{4\sqrt{\varepsilon_r}} \tag{3}$$

where λ_0 is the wavelength at the operating center frequency in free space. Using Eq. (3) we find the required length of the transverse slot to be 2.2 mm. However, as can be seen in Fig. 2(b), if the transverse slot is etched at an angle perpendicular to the direction of transmission ($\theta_s = 90°$), an impedance mismatch in a narrow operating bandwidth will remain. This is because the real part of impedance of the etched vertical slot is greater than 85 Ω near 24 GHz, which is not impedance matched with the microstrip feed line. To obtain good impedance matching, we optimize the slot angle relative to the transmission direction. Rotating the transverse slot 28° counterclockwise (such that $\theta_s = 118°$), we find the real and imaginary parts of the unit-cell impedance to be about 50 and 0 Ω, respectively, throughout the radiating region (i.e., above 18 GHz), which fully eliminates the stopband, as can be seen in Fig. 2(a).

The full LWA consists of matched unit-cells cascaded along the direction of propagation (y-axis), and two microstrip lines loaded as the feed line. For the full LWA, the attenuation (leakage) constant and radiation efficiency should be considered to further analyze the transmission and radiation performance. The attenuation constant as a function of frequency represents the radiation per length for the two-port LWA, and can be calculated using the $ABCD$ parameters and S-matrix according to:

$$\alpha = \frac{1}{L}\mathrm{In}\left|A \pm \sqrt{A^2 - 1}\right| \tag{4}$$

$$\alpha = \frac{-1}{2L}\mathrm{In}\frac{|S_{21}|^2}{1 - |S_{11}|^2} \tag{5}$$

$$R_{Se} = 1 - \exp(-2\alpha L) = \frac{1 - |S_{11}|^2 - |S_{21}|^2}{1 - |S_{11}|^2} \tag{6}$$

where L is the length of the leaky structure [16], [18], and R_{Se} is the radiation efficiency. It should be noted that the S-parameter-based radiation efficiency, R_{Se}, only describes the radiation performance from power transmission. Thus, as the directivity of LWA is relatively high, the radiation efficiency obtained from the simulations, R_e, that takes into account antenna directivity and gain needs to be considered. The normalized attenuation constant, α/k_0, the S-parameter-based radiation efficiency, R_{Se}, and the simulated radiation efficiency, R_e, are plotted in Fig. 3. As can be seen, the value of normalized attenuation constant is smooth and close to 0 in K-band, clearly demonstrating that there is no stopband in the operating bandwidth and the S-parameter-based radiation efficiency is larger than 40% in the operating bandwidth with a maximum value of 60% at 23 GHz. Furthermore, the simulated radiation efficiency is high with an average of 86% and a maximum of 92% at 23 GHz, which confirms that the matched broadband full LWA concentrates most of the power on the main beam direction.

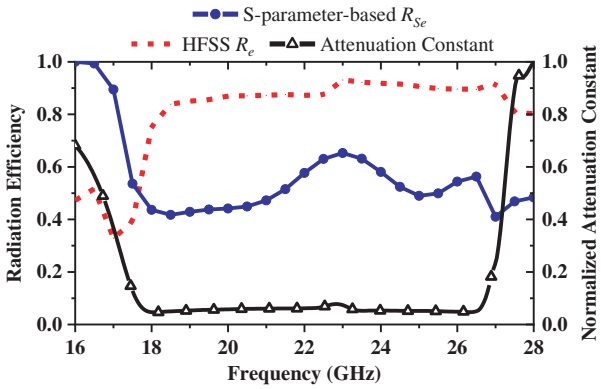

Figure 3. Simulated HFSS radiation efficiency (R_e), S-parameter-based radiation efficiency (R_{Se}) and normalized attenuation (leakage) constant for the proposed LWA.

3. FABRICATION AND CHARACTERIZATION

A prototype of the antenna with fifteen unit-cells, shown in Fig. 4, was fabricated and characterized for verification of the design. Due to the softness of the antenna substrate, an acrylic clamp is placed at the bottom of the antenna and fixed with acrylic screws to facilitate measurements. To ensure easy assembly, the LWA ports are connected by two end launch connectors and we furthermore use a grounded coplanar waveguide (GCPWG) structure to ensure that the ground of the antenna is well connected to the outer conductor of the end launch connectors. An Agilent N5247A network analyzer is used to measure the S-parameters of the fabricated LWA, which are plotted together with the simulated S-parameters in Fig. 5. The measured impedance bandwidth (defined as the band where S_{11} is below -10 dB) is 17.6 GHz to 28 GHz, which covers the whole K-band. This is slightly wider than the simulation result (17.8 GHz to 27.2 GHz), which we attribute to fabrication errors. Measured S_{21} values are slightly lower than the simulation results, which can be attributed to the loss in the connectors and cables. Note that the sum of the return loss and insertion loss is less than 1 due to some internal losses (including dielectric and conductor losses) in the leaky structure and the external loss caused by the radiation in the actual antenna model. For the LWA gain measurement, one antenna port is terminated by a 50 Ω load. Fig. 6 shows the simulated and measured normalized radiation patterns and realized gain in the K-band frequency range. The measured radiation patterns demonstrate continuous beam scanning from $-34°$ to $+22°$, in accordance with the simulation results. The measured realized gain is between 0.6 dB (at 22 GHz) to 3.1 dB (at 18 GHz) and the maximum gain is 15.8 dBi, which is lower than the simulation result due to the loss in the adaptors and fabrication errors. The maximum gain is 15.8 dBi at 22 GHz, which has some shift compared with the simulated result (25 GHz) (we believe this is mainly due to the dispersion of the dielectric constant and loss tangent of the used substrate). However, all measurement results demonstrate that the proposed LWA has good free space radiation characteristics.

Our proposed LWA thus exhibits excellent performance in terms of realized gain and impedance bandwidth. Comparison of key parameters with previously reported work is merited and we summarize this in Table 2. The CP LWA based on a CSIW in [13] has a very limited scanning range and the

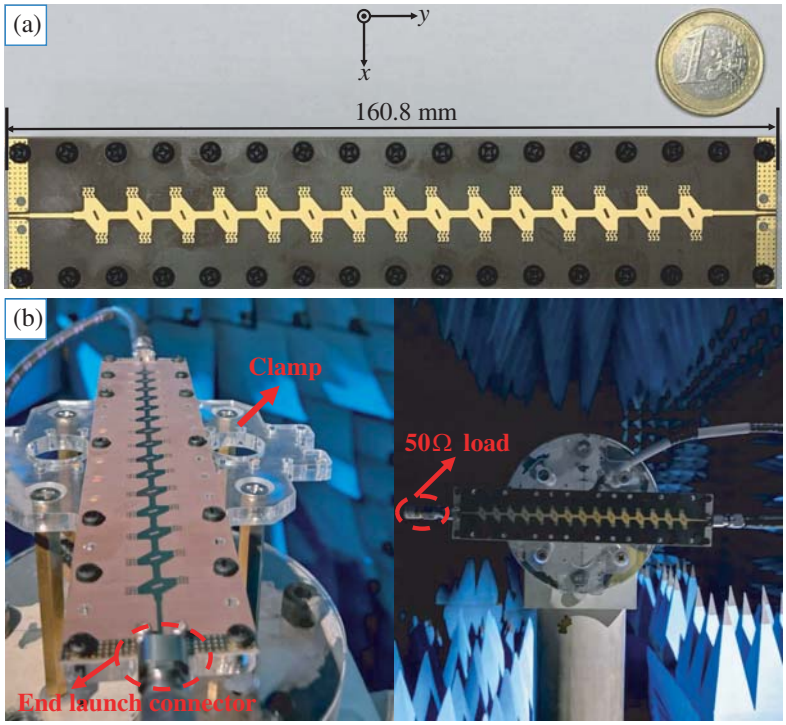

Figure 4. (a) Fabricated prototype of the proposed LWA. (b) Setup for LWA gain measurement in an anechoic test chamber.

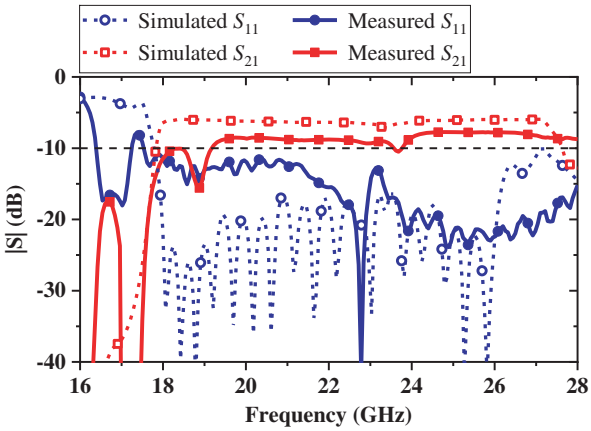

Figure 5. Simulated and measured S-parameters of the proposed LWA.

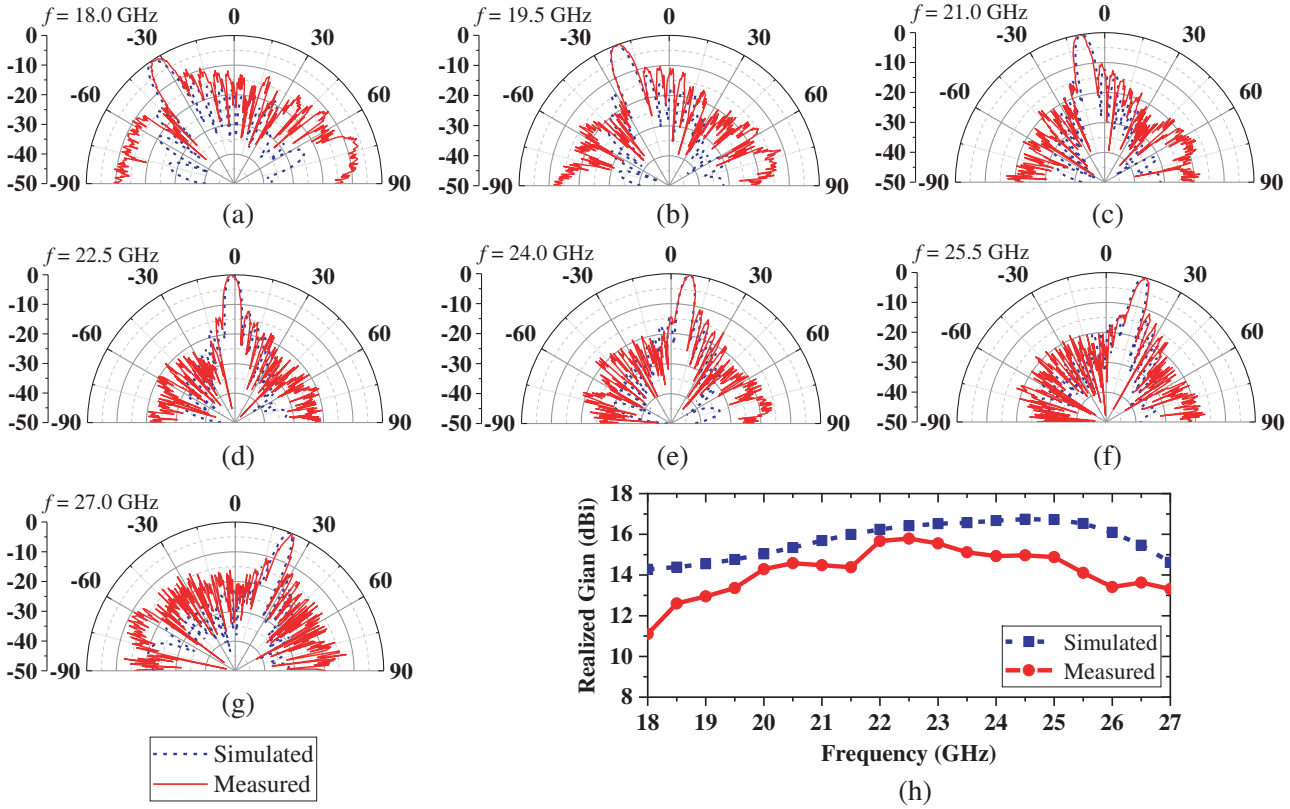

Figure 6. Simulated and measured normalized radiation patterns of the proposed LWA: (a) 18.0 GHz, (b) 19.5 GHz, (c) 21.0 GHz, (d) 22.5 GHz, (e) 24.0 GHz, (f) 25.5 GHz, (g) 27.0 GHz. (h) Simulated and measured realized gain of the proposed LWA in the K-band.

antenna width ($0.97\lambda_0$) is 10.3% wider than that of the LWA in this work ($0.87\lambda_0$). The width of the LWA presented here is also 6.5% less than that of our previously reported LWA [14]. As is evident from Table 2, the bandwidth and scanning range of the LWA proposed here are improved compared to Refs. [7–9, 13]. Furthermore, compared with LWAs with etched single transverse slot radiators [7–9, 14], our design enables backward to forward beam scanning through the combination of two different types of radiators. In particular, besides more compact structure, the present LWA has much larger bandwidth (45.6%) than our earlier work [14] (28.1%).

Table 2. Comparison of the LWA proposed in this paper with previously reported LWAs.

Ref.	[13]	[9]	[8]	[7]	[14]	Our work
Radiator & Type	Compound Slot Pair CSIW	Transverse Slot SIW	Transverse Slot SIW	Transverse Slot SIW	Transverse Slot BCSIW	Edge & Transverse Slot S-shaped Folded CSIW
Pol.	CP	LP	LP	LP	LP	LP
Bandwidth (GHz)	16.2–16.8 (3.6%)	15.8–19.4 (20.45%)	14.8–15.5 (4.6%)	10.2–12 (16.2%)	22–29.2 (28.1%)	17.6–28 (45.6%)
Gain (dBi)	/	$> 18^*$	7	12	16.2	15.8
Size (λ_0)	$7.9 \times 0.97 \times 0.08$	$18.6 \times 0.76 \times 0.05$	$9.5 \times 0.97 \times 0.08$	$12 \times 0.48 \times 0.06$	$13 \times 0.95 \times 0.04$	$12 \times 0.87 \times 0.02$
Scanning Range	$(-90°, -87°)$ $3°$	$(-131°, -99°)$ $32°$	$(-54°, -40°)$ $13°$	$(-70°, -20°)$ $50°$	$(-69°, -10°)$ $59°$	$(-34°, +22°)$ $56°$

*: Simulated Result.

4. CONCLUSION

In this paper we have introduced a novel periodic leaky-wave antenna (LWA) based on a corrugated substrate integrated waveguide (CSIW). The design includes two separate types of radiator elements, parallel edges as well as a transverse slot with a tilt angle, and enables a large scanning angle range from backward to forward radiation over a large frequency range. By including S-shaped quarter-wavelength microstrip lines in the unit-cell the total length of the LWA has been significantly reduced. Additionally, the S-shaped stubs ensure a more compact CSIW structure as compared with traditional CSIW structures. We have verified the design experimentally by characterizations of a fabricated protype. Measurement results have shown that the impedance bandwidth of the LWA covers the full K-band frequency range, and has a scan angle from $-34°$, $+22°$ with a peak gain of 15.8 dBi. Our proposed LWA is a promising candidate for millimeter wave devices and systems.

ACKNOWLEDGMENT

This work was supported in part by Ningbo Science and Technology (project No. 2018B10093), the National Key Research and Development Program of China (No. 2018YFC1407503), the National Natural Science Foundation of China (under Grants 61774131 and 11621101), and partially the Science and Technology Cooperation project of Guizhou Province in 2017 (No. Qiankehe LH [2017]7322).

REFERENCES

1. Yi, Z., et al., "A wide-angle beam scanning antenna in *E*-plane for K-band radar sensor," *IEEE Access*, Vol. 7, 171684–171690, 2019.
2. Moon, S., S. Yun, I. Yom, and H. L. Lee, "Phased array shaped-beam satellite antenna with boosted-beam control," *IEEE Trans. Antennas Propag.*, Vol. 67, No. 12, 7633–7636, Dec. 2019.
3. Jackson, D. R., C. Caloz, and T. Itoh, "Leaky-wave antennas," *Proc. IEEE*, Vol. 100, No. 7, 2194–2206, Jul. 2012.
4. Mohsen, M. K., M. S. M. Isa, A. A. M. Isa, M. K. Abdulhameed, M. L. Attiah, and A. M. Dinar, "Enhancement bandwidth of half width-microstrip leaky wave antenna using circular slots," *Progress In Electromagnetics Research C*, Vol. 94, 59–74, 2019.

5. Hyneman, R. F., "Closely-spaced transverse slots in rectangular waveguide," *IRE Trans. Antennas Propag.*, Vol. 7, No. 4, 03–42, Oct. 1959.
6. Liu, J., D. R. Jackson, and Y. Long, "Modal analysis of dielectric-filled rectangular waveguide with transverse slots," *IEEE Trans. Antennas Propag.*, Vol. 59, No. 9, 3194–3203, Sep. 2011.
7. Liu, J., D. R. Jackson, and Y. Long, "Substrate integrated waveguide (SIW) leaky-wave antenna with transverse slots," *IEEE Trans. Antennas Propag.*, Vol. 60, No. 1, 20–29, Jan. 2012.
8. Geng, Y., J. Wang, Z. Li, Y. Li, M. Chen, and Z. Zhang, "A leaky-wave antenna array with beam-formed radiation pattern for application in a confined space," *IEEE Access*, Vol. 7, 86367–86373, 2019.
9. Javanbakht, N., M. S. Majedi, and A. R. Attari, "Periodic leaky-wave antenna with transverse slots based on substrate integrated waveguide," *2016 24th Iranian Conference on Electrical Engineering (ICEE)*, 608–612, Shiraz, Iran, May 2016.
10. McMillan, L. O., N. V. Shuley, and P. W. Davis, "Leaky fields on microstrip," *Progress In Electromagnetics Research*, Vol. 17, 323–337, 1997.
11. Lee, H., J. H. Choi, C.-T. M. Wu, and T. Itoh, "A compact single radiator crlh-inspired circularly polarized leaky-wave antenna based on substrate-integrated waveguide," *IEEE Trans. Antennas Propag.*, Vol. 63, No. 10, 4566–4572, Oct. 2015.
12. Eccleston, K. W., "Mode analysis of the corrugated substrate integrated waveguide," *IEEE Trans. Microwave Theory Techn.*, Vol. 60, No. 10, 3004–3012, Oct. 2012.
13. Liu, C., Z. Li, and J. Wang, "A new kind of circularly polarized leaky-wave antenna based on corrugated substrate integrated waveguide," *Proc. IEEE 5th Int. Symp. Microw., Antenna, Propag. EMC Technol. Wireless Commun. (MAPE)*, 383–387, Oct. 2013.
14. Lin, Y., Y. Zhang, H. Liu, Y. Zhang, E. Forsberg, and S. He, "A simple high-gain millimeter-wave leaky-wave slot antenna based on a bent corrugated SIW," *IEEE Access*, Vol. 8, 91999–92006, 2020.
15. Chen, K., Y. H. Zhang, S. Y. He, H. T. Chen, and G. Q. Zhu, "An electronically controlled leaky-wave antenna based on corrugated SIW structure with fixed-frequency beam scanning," *IEEE Antennas Wireless Propag. Lett.*, Vol. 18, No. 3, 551–555, Mar. 2019.
16. Caloz, C. and T. Itoh, *Electromagnetic Metamaterials: Transmission Line Theory and Microwave Applications*, Wiley, Hoboken, NJ, USA, 2005.
17. Sarkar, A., M. Adhikary, A. Sharma, A. Biswas, M. J. Akhtar, and Z. Hu, "Composite right/left-handed based compact and high gain leaky-wave antenna using complementary spiral resonator on HMSIW for Ku band applications," *IET Microw. Antennas Propag.*, Vol. 12, No. 8, 1310–1315, 2018.
18. Sabahi, M. M., A. A. Heidari, and M. Movahhedi, "A compact CRLH circularly polarized leaky-wave antenna based on substrate-integrated waveguide," *IEEE Trans. Antennas Propag.*, Vol. 66, No. 9, 4407–4414, Sep. 2018.
19. *Left-handed Metamaterial Design Guide*, Ansoft Corp., Pittsburgh, PA, USA, 2007.
20. Agrawal, R., P. Belwal, M. Singh, and S. C. Gupta, "Continuous beam scanning in substrate integrated waveguide leaky wave antenna," *Progress In Electromagnetics Research M*, Vol. 62, 19–28, 2017.
21. Liu, J., W. Zhou, and Y. L. Long, "A simple technique for open-stopband suppression in periodic leaky-wave antennas using two nonidentical elements per unit cell," *IEEE Trans. Antennas Propag.*, Vol. 18, No. 2, 353–357, Jun. 2019.